ELSEVIER

Tectonophysics 280 (1997) 31–45

TECTONOPHYSICS

Analysis of a complex high-strain zone at Cap de Creus, Spain

E. Druguet [a,*], C.W. Passchier [b], J. Carreras [a], P. Victor [b], S. den Brok [b]

[a] *Departament de Geologia, Universitat Autònoma de Barcelona, 08193 Bellaterra, Barcelona, Spain*
[b] *Institut für Geowissenschaften, Universität Mainz, Mainz, Germany*

Received 27 February 1996; accepted 29 October 1996

Abstract

The structural analysis of a high-strain zone developed in medium- to high-grade metamorphic micaschists from the Cap de Creus area, Spain provides an example of the complex relationships between geometry, strain and kinematics to be found in deep crustal shear zones. This high-strain zone is composed of E–W trending structural domains characterized by different strain intensities and associated with syntectonic emplacement of pegmatite dykes. The main phase of deformation discussed here, D_2, affects steeply dipping bedding, boudinaged quartz veins and S_1 developed parallel to bedding. D_2 deformation of these features and of syn-D_2 pegmatite dykes gives rise to fold/boudin structures. In map view, a D_2 high-strain zone coincides with a km-scale dextral flexure of S_0, S_1 and S_2, although all small-scale structures on outcrop surfaces close to horizontal indicate a prevalent sinistral shear sense. In addition, a subvertical stretching lineation is present approximately parallel to the axis of the foliation-deflection and thus normal to the apparent 'displacement' direction in the high-strain zone. It is proposed that this high-strain zone did not form by horizontal dextral simple shear with a flow plane parallel to the boundaries of high- and low-strain zones but acted as a zone of highly vortical sinistral non-coaxial flow with a strong vertical extension component. The dextral flexure of S_0, S_1 and S_2 can be explained by considering that sinistral non-coaxial flow in the low-strain zones was either slower or earlier that in the high-strain core. This example stresses the necessity of being careful when interpreting displacement directions from the deflection of older fabric elements in deep-seated high-strain zones.

Keywords: strain analysis; kinematics; deformed veins; Pyrenees

1. Introduction

High-strain zones that formed at deep crustal levels have received increasing attention in the literature because of their common association with synkinematic igneous intrusions (Reavy, 1989; Ingram and Hutton, 1994; McCaffrey, 1994; Karlstrom and Williams, 1995). Deep crustal high-strain zones differ in many aspects from well-known greenschist facies upper crustal shear zones (e.g. Ramsay, 1980; Passchier and Trouw, 1995). In deeper high-strain zones, deformation is not by plane strain flow, and volume changes associated with igneous intrusion and partial melting is more common. In some cases, even the familiar parallel relationship between stretching lineations and displacement direction (Ramsay, 1980), common in low- and medium-grade mylonites, is absent, and lineations may appear to lie oblique to the displacement direction of the

* Corresponding author. Fax: +34-3-581-1263; E-mail: geotec@geologia.uab.es.

PII S0040-1951(97)00137-6

shear zone (Robin and Cruden, 1994). It is important to characterize deformation in such high-strain zones in order to reconstruct the tectonic regimes operating in the crust and to interpret associated processes like magma emplacement.

In this paper, an example is given of a high-strain Hercynian deformation zone with an unusual deformation pattern and history in medium to high-grade micaschists and associated syntectonic pegmatite dykes from the Cap de Creus area (Spain). The combined analysis of strain in the country rock and strain recorded by differently oriented syntectonic dykes gives information on the deformation history and puts constraints on the type of deformation involved. A model invoking progressive deformation and strain heterogeneization is proposed.

2. Geological setting

The Cap de Creus area, Spain, consists mainly of alternating metapsammitic (metagreywackes) and minor metapelitic rocks of Neoproterozoic to Ordovician age. Several isolated layers of quartzite, up to 3 m wide have been recognised and can be used as tracers for large-scale structures in the area. The area is affected by a polyphase tectonics with at least two deformation events during the prograde low-pressure Hercynian regional metamorphism and late shearing events in retrograde conditions. Metasediments show a gradient from the chlorite–muscovite zone in the south to the sillimanite–K feldspar zone in the north. Locally, migmatites were formed along the northern coastline of the Cap de Creus peninsula (Druguet et al., 1995). Medium grade micaschists in the northern part of the area are extensively intruded by pegmatite dykes (Carreras and Druguet, 1994).

The oldest deformation in the area (D_1) led to the development of a first continuous and penetrative schistosity (S_1) in the metasediments, formed prior to the metamorphic climax. A few isoclinal D_1 folds have been found in the area and, with the exception of these structures, S_1 is subparallel to S_0 throughout the area. For this reason, the orientation of both structures is described in this paper as $S_{0/1}$. Numerous quartz veins (from 1 mm to 50 cm wide) of D_1 age or older, were deformed during D_1 and developed boudins and a marked stretching lineation.

Later intense and inhomogeneous D_2 deformation led to folding of bedding, S_1 and quartz veins, with upright or steeply inclined axial surfaces which trend approximately NE–SW in less deformed areas and E–W in more deformed areas. D_2 structures formed around the time when peak metamorphic conditions were reached, as shown by the presence of synkinematic sillimanite and 1–10 cm long partial melt veins. Pegmatite dykes, some of them muscovite, sillimanite and garnet bearing, intruded after the peak of metamorphism. The intrusion apparently took place during D_2. Temperatures of crystallization are estimated over 580°C (Alfonso, 1995).

A last major deformation event, D_3, gave rise to E–W to NW–SE trending anastomosed ductile shear zones developed under retrograde metamorphic conditions (Carreras and Casas, 1987). Mylonitic bands in the Cap de Creus area are related to this anastomosed network of late shear zones, cutting across medium–high-grade schists and pegmatites, with predominantly dextral strike-slip or oblique-slip movements.

This paper describes the results of detailed analysis of structures developed during the prograde stage (D_1 and D_2) in medium to high-grade domains in an area of the Cap de Creus Peninsula (Fig. 1).

3. D_2 structures

The structures generated during D_2 are the principal subject of this paper and were investigated in detail in the area outlined in Fig. 1. This area is located in the medium- to high-grade metamorphic zone mainly formed by sillimanite-bearing micaschists. In this area, D_2 deformation was heterogeneously distributed and three structural domains with relatively high- and low-D_2 strain can be distinguished (Fig. 2). The low-strain domains are characterised by a subvertical nearly N–S trending $S_{0/1}$. In these domains D_2 folds are open and the associated crenulations develop exclusively in more pelitic schists. Strain-increase towards the high-strain zone is accompanied by the development of 'S'-shaped D_2 folds in bedding on a 10 cm–100 m scale with an associated subvertical crenulation cleavage (S_2). These folds are most common near pegmatite dykes, probably due to inhomogeneous deformation induced by the presence of these dykes. The D_2 folds have subvertical or steeply plunging axes (Fig. 2), which are

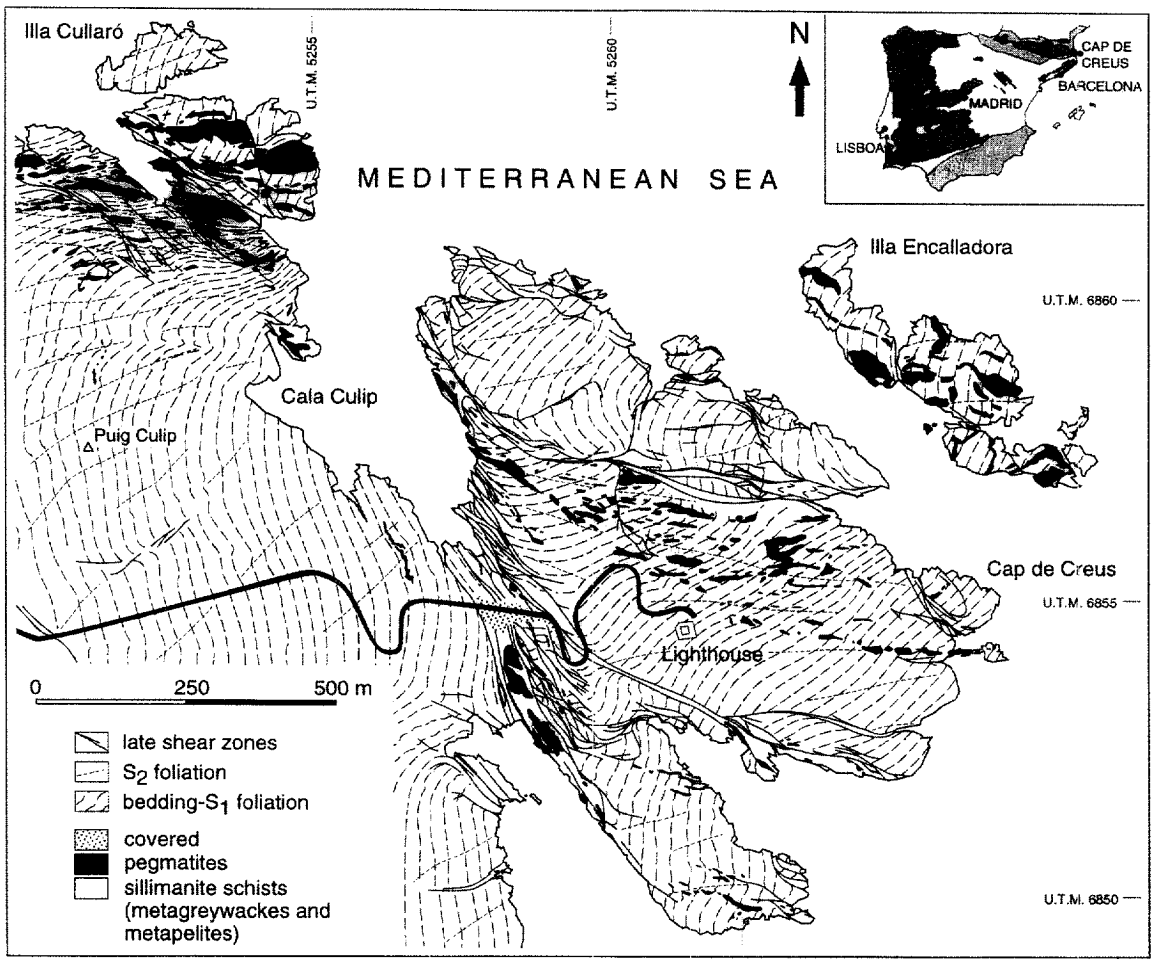

Fig. 1. Structural map of the Culip–Cap de Creus area.

closely parallel to equally steeply inclined lineations. Most lineations are L_2-lineations, usually stretching lineations defined by elongate quartz grains, and mineral lineations defined by sillimanite, tourmaline or biotite. These lineations are mainly developed in the deformed pegmatite dykes described below, but locally also in quartz veins and bedding. L_2^1 or L_2^0 intersection lineations also occur and are parallel to L_2 throughout the low-strain domain. D_2 folds are cylindrical with axes subparallel to these lineations.

Towards the centre of the high-strain zone, a further increase in strain is manifested by the increasing tightness of D_2 folds and a change in the general orientation of $S_{0/1}$ and S_2 towards a steeply dipping NE–SW or even E–W trend. Also, the angle between $S_{0/1}$ and S_2 decreases with increasing D_2 strain from 39° in the low-strain areas up to subparallelism in the centre of the highest strain zone (Fig. 2). The change in orientation of both foliations from the low-strain into the high-strain zone defines a cylindrical sigmoidal structure, with axes parallel to D_2 lineations and fold axes (Figs. 2 and 3; fig. 5 in Carreras and Druguet, 1994). In a section across the high-strain zone from southern low-strain zones to the north, the abundance of andalusite porphyroblasts decreases, the density and size of pegmatite dykes and the size of sillimanite grains increases. This suggests that the high-strain zone formed at medium to high-grade metamorphic conditions, like D_2 structures in the low-strain zones. The change in orientation of S_2

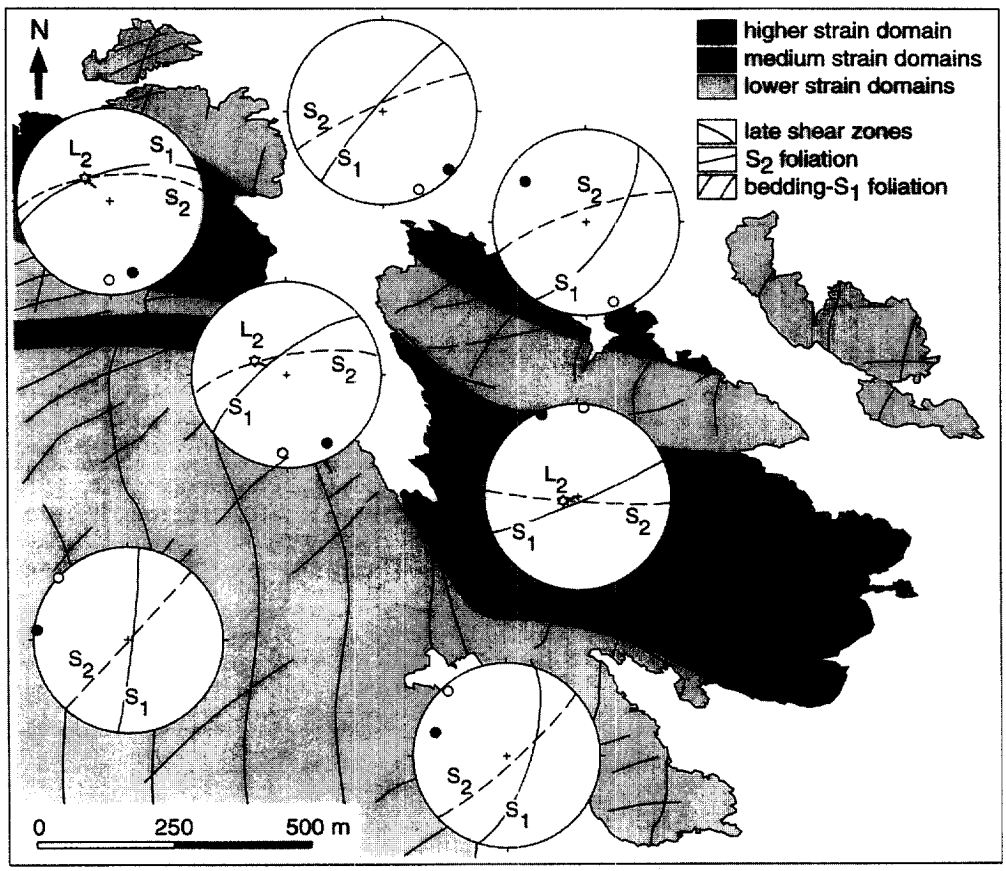

Fig. 2. Sketch map of the Culip–Cap de Creus area showing the arrangement of different structural domains and their equal-area lower-hemisphere stereoplots. Main great circles of S_1 and S_2 and its poles (S_1 in black and S_2 in white) are shown. L_2 = mean values of stretching lineations from medium- to high-strain zones.

towards the high-strain zone does not appear to be the effect of deformation later than D_2, since folds and their related axes and crenulation cleavages are undisturbed by later deformation phases except in the vicinity of greenschist-facies D_3 shear zones.

3.1. Sigmoidal quartz-rods

Early quartz-veins were emplaced throughout the area prior to the development of D_2 folds. These veins usually have millimetre to centimetre thicknesses and display D_2 boudinage or folding structures (Fig. 4a) depending on their original orientation. Some of them were boudinaged before the onset of D_2, developing into a peculiar shape during D_2 as a result of general shortening of the veins and rotation of the boudins by D_2. These structures, here designed as sigmoidal quartz-rods, develop an asymmetric shape on horizontal surfaces with the widest part of the boudins at an angle to the nearly undisturbed $S_{O/I}$ in the wall of the rock, even in the absence of D_2 folding (Fig. 4b,c). The angle of obliqueness between these quartz-veins structures and $S_{O/I}$ plane varies from 0° to 170°(anti-clockwise sense). Short, stocky boudins develop a shape resembling δ-shaped mantled porphyroclasts (Fig. 4c). Where S_2 is present, its orientation in the embayments of the quartz-vein structures makes a larger angle with $S_{O/I}$ than in the wall rock, suggesting lower strain in these domains. $S_{O/I}$ is usually straight in the wall rock and wraps around the sigmoidal quartz-rods. Throughout the area, in high- and low-

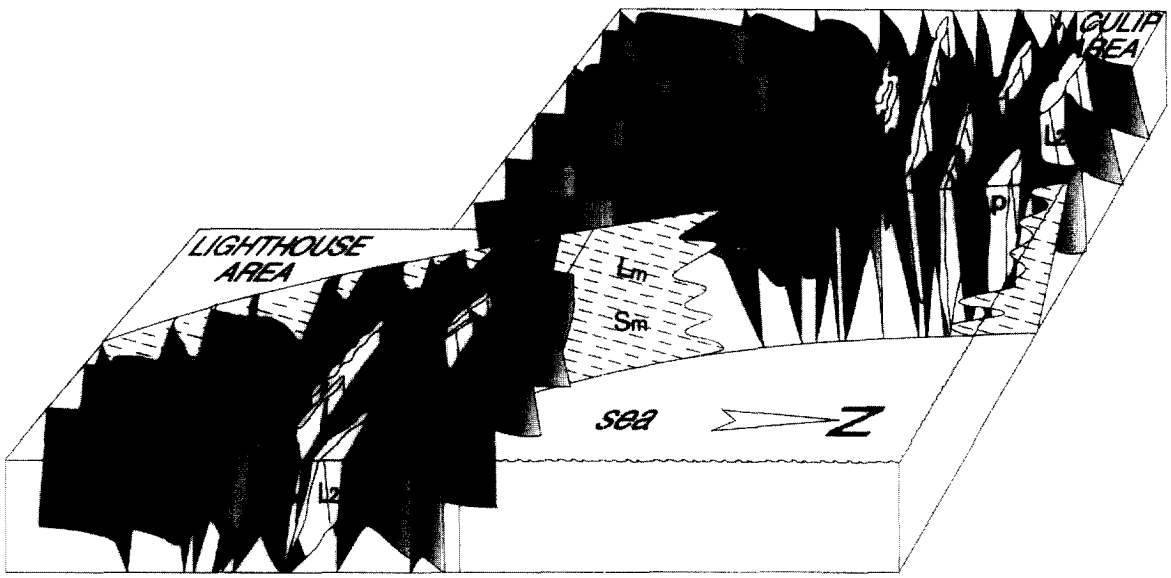

Fig. 3. Schematic block diagram showing the three-dimensional arrangement of the main structural elements in the area. For the sake of simplicity only one late shear zone separating the Culip and the Lighthouse areas is represented. $S_{0/1}$ = bedding and bedding parallel foliation, S_2 = crenulation cleavage, L_2 = D_2 related stretching lineations, *Sm* and *Lm* are respectively the mylonitic foliation and the associated stretching lineation, *p* = pegmatites.

strain zones, sigmoidal quartz-rods have an S-geometry on horizontal pavements. In three dimensions the structures are highly cylindrical with the symmetry axis parallel to D_2 stretching or intersection lineations. Sigmoidal quartz-rods on a 10-cm scale of identical geometry and vergence are present in both limbs of 10 metre-scale D_2 folds, showing that folding locally postdated the development of sigmoidal quartz-rods and that they are not simply small-scale D_2 folds.

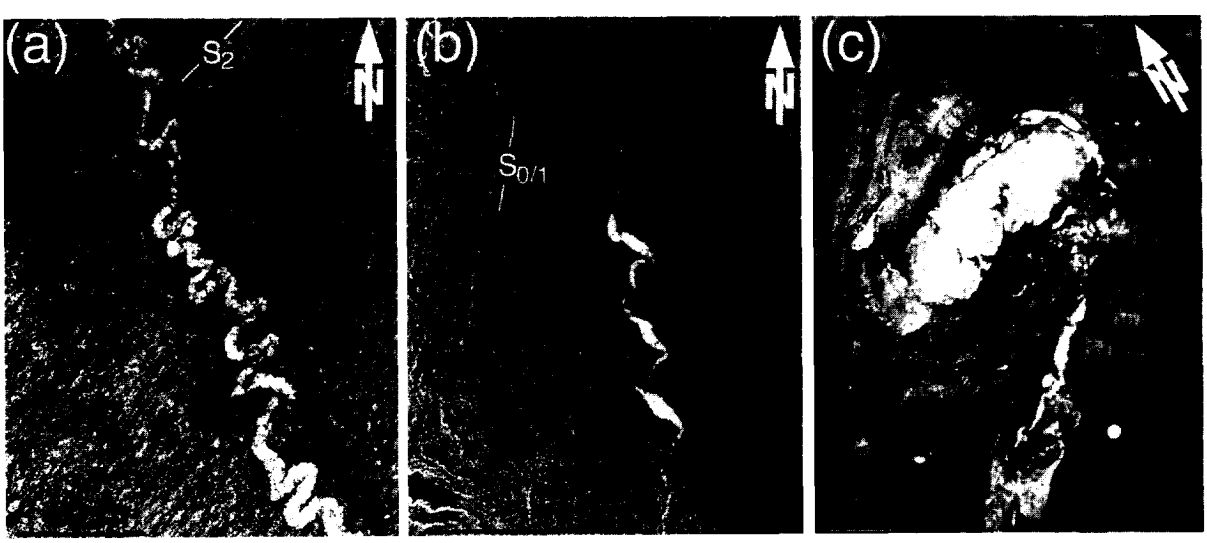

Fig. 4. Field photographs of quartz-veins. All sections are plane view. (a) D_2 folded quartz-vein, highly oblique to S_2 crenulation cleavage. (b) Sigmoidal quartz-rods displaying asymmetric shapes. (c) sigmoidal quartz-rod with a shape similar to a δ-object.

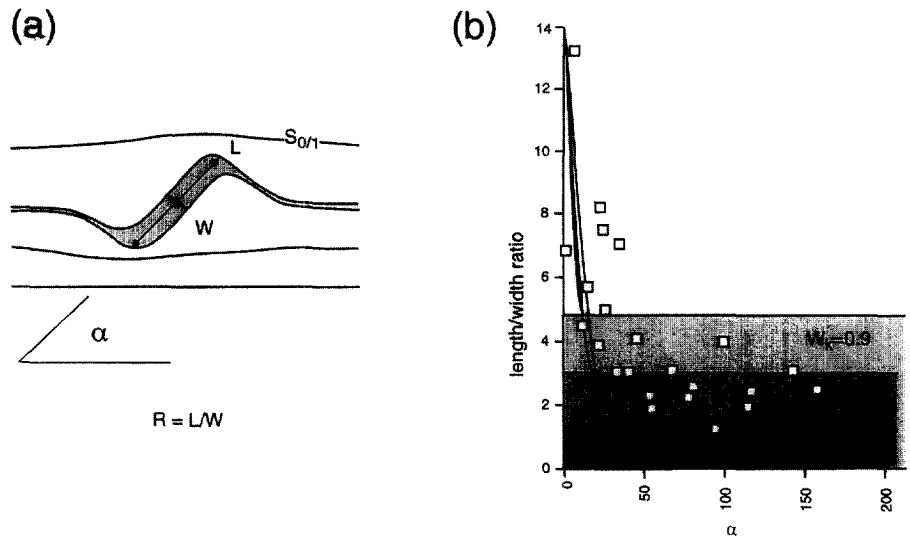

Fig. 5. The length–width ratio R and orientation α with respect to the $S_{O/1}$ of sigmoidal quartz-rods can be determined as shown in (a). In (b), a plot of R against α shows small rotation angles at high R (>4.5) and high rotation angles above this value. The theoretical orientation of rigid ellipses for the kinematic vorticity number (Means et al., 1980) $W_k = 0.9$, 0.8 and 0.5 is indicated for comparison; at low R the ellipses can rotate freely (grey domains), while at high R over a certain critical value they lie in a blocked position along one of the curves for the respective. Although the fit is poor, since quartz vein structures are not isolated rigid ellipses, the distribution of R/α values with respect to the graphs suggests that W_k is relatively high, near $W_k = 0.9$.

The proposed interpretation of the sigmoidal quartz-rods is as follows. The massive D_1-boudins in quartz veins acted as relatively competent bodies during D_2 flow. The geometry of the sigmoidal quartz-rods indicates that they formed by relative rotation of the massive boudins over variable angles with respect to $S_{O/1}$. Most likely, the structures formed in sinistral non-coaxial flow; this would cause round objects to rotate permanently, stocky competent objects to rotate over a certain angle, while more elongate bodies such as $S_{O/1}$ and pegmatite veins are blocked in rotation (Passchier, 1987); (Fig. 5).

Porphyroblasts of andalusite up to 5 cm diameter occur all over the study area. S_1 is deflected around these andalusites but is continuous inside them with straight inclusion patterns S_i. Most porphyroblasts have an oblique-S_i geometry (Passchier and Trouw, 1995) i.e. S_i differs in orientation from S_1 in the wall rock. This structure shows that andalusite grew intertectonic between D_1 and D_2 (Passchier and Trouw, 1995, chapter 7). Anti-clockwise rotation in the map view and 'northern block down' in the vertical section seem dominant.

3.2. Pegmatite dykes

In map view (Fig. 1), a pegmatite dyke swarm occurs in the area in a band closely parallel to the trend of the higher strain zone, although some dykes also intrude more marginal, less deformed domains. Pegmatites mainly form planar dykes up to 5 m wide, but also more irregularly shaped elongate bodies up to a few hundred meters long and 40 m wide (Fig. 1). Pegmatites are subvertical and range in orientation from orthogonal to nearly subparallel to $S_{O/1}$ (Fig. 3). The intersection lineation of pegmatite dykes with $S_{O/1}$ and S_2 and the intersection lineation of both foliations are all subparallel. Some subhorizontal or gently dipping pegmatite dykes up to 1 m thick and 100 metres long are also present in the high-strain zone (Fig. 6), and these are connected to vertical pegmatite veins which seem to have acted as feeder dykes.

Most pegmatites are folded or boudinaged during D_2 (Fig. 7a,b), and S_2 is associated with the development of these structures. D_2 folds in pegmatites are coaxial with D_2 folds in $S_{O/1}$ but are more open. (Fig. 8). Folding may have taken place when the pegmatite dykes were still partly liquid. Cuspate–lobate

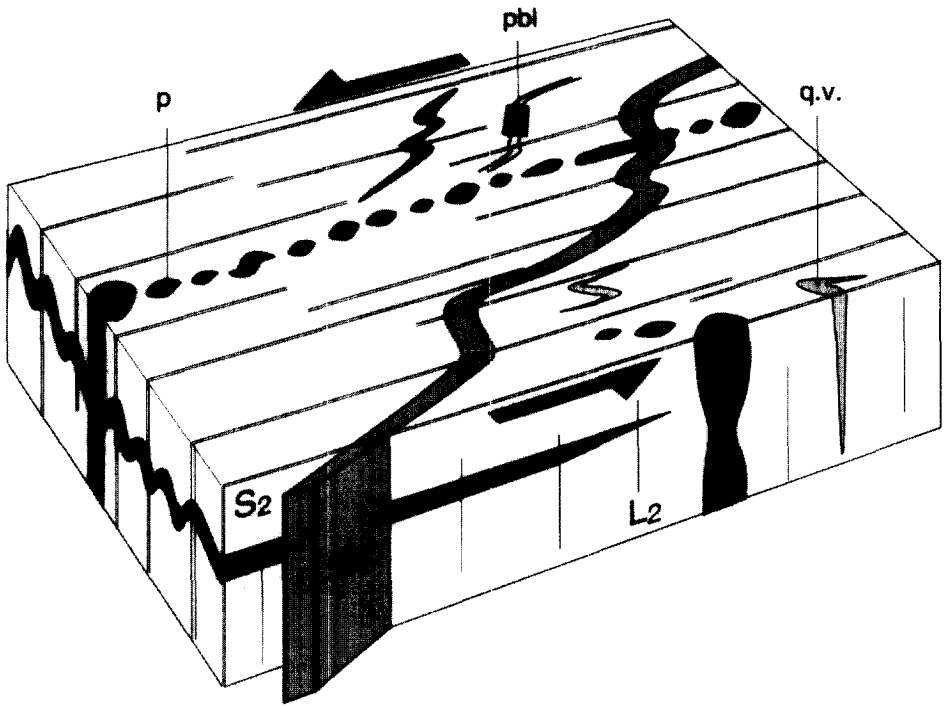

Fig. 6. Scheme showing different shear sense markers (*q.v.* = quartz veins, *pbl* = porphyroblasts). Pegmatite dykes (*p*) closely parallel to S_2 exhibit boudinage, while $S_{O/1}$-parallel dykes are folded. Some steep pegmatites have subhorizontal branches which become folded during D_2.

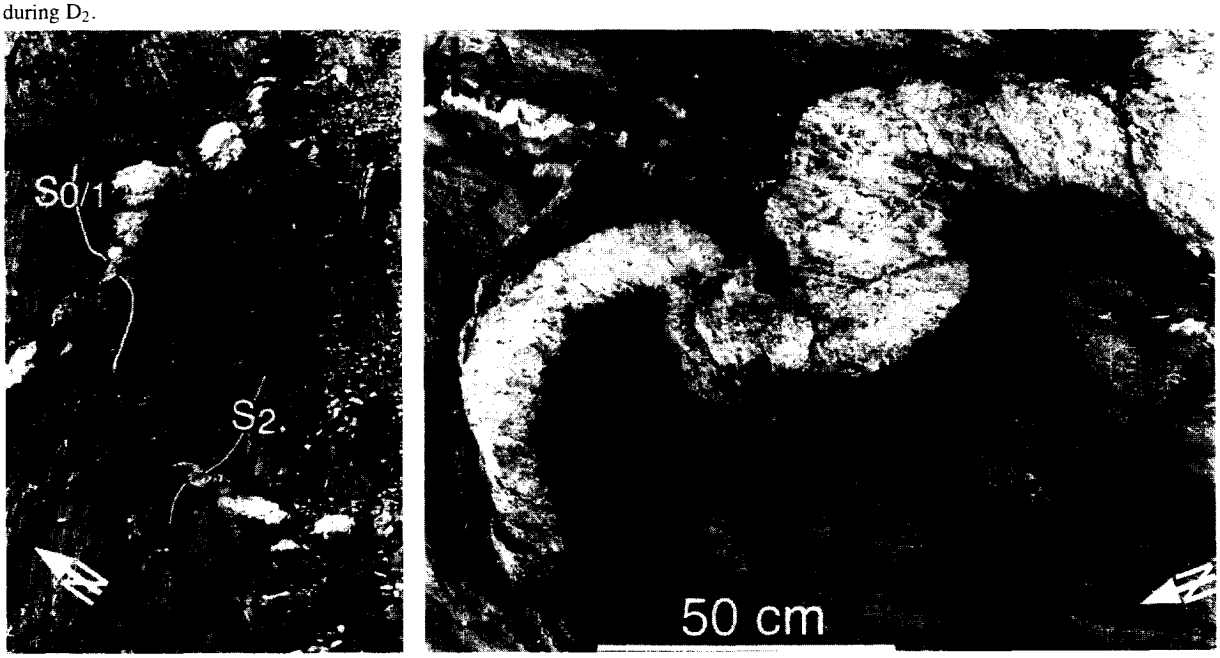

Fig. 7. Field photographs of pegmatite structures. All sections are plane view and the location is shown in Fig. 13. (a) Boudinaged (above) and folded (below) pegmatite dykes from the medium strain domain, used to determine sectional strain ellipse in Fig. 12. (b) Detailed view of the folded pegmatite. Note its obliquity with respect to both $S_{O/1}$ and S_2 foliations.

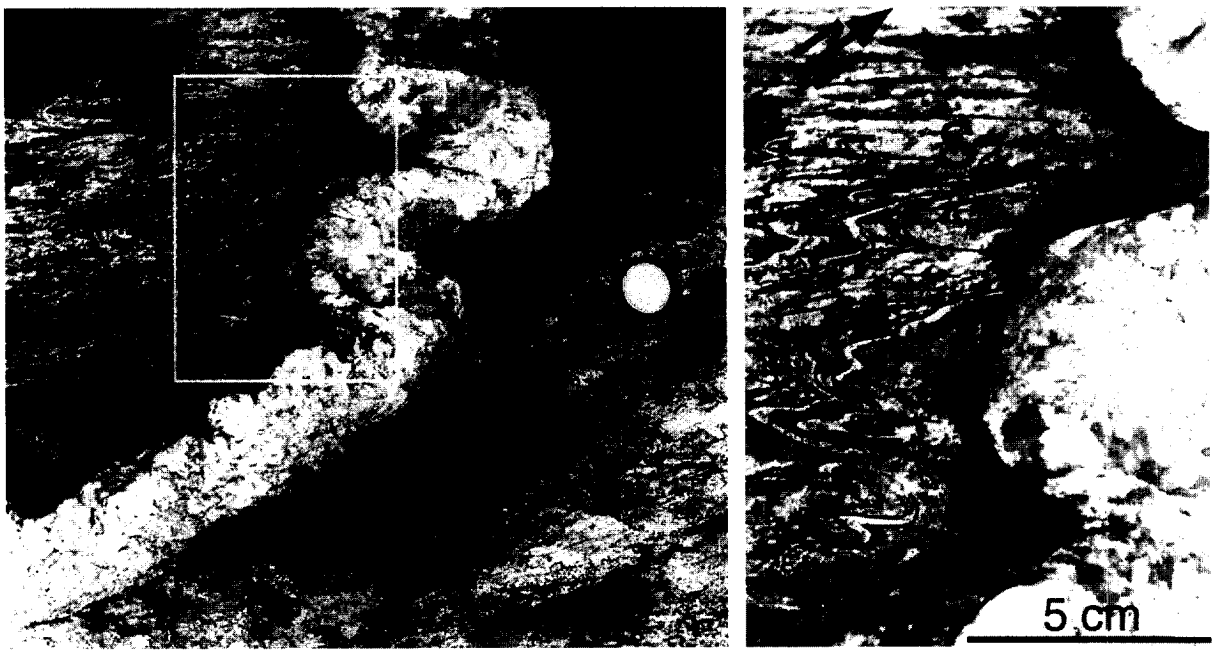

Fig. 8. Field photograph and detail sketch of a D_2 synmagmatically folded pegmatite vein. Folds in schists and pegmatite are coaxial but differ in tightness. Section is close to horizontal.

structures around the folded pegmatites indicate a more competent behaviour of the magmatic crystal mush than the enclosing metasediments. A non-penetrative solid state tectonic fabric is present in most of the pegmatites although some pre-full crystallization fabrics (Hutton, 1988) and compositional banding parallel to S_2 are occasionally observable. Some pegmatites, deformed by D_2, are seen to cut both S_2 and D_2 folds affecting $S_{O/I}$ and quartz veins. Therefore, pegmatite intrusion seems clearly synkinematic with D_2 deformation (Carreras and Druguet, 1994).

Boudinaged dykes also develop complex structures. Boudinage either develop pinch-and-swell features, or separated boudins connected by thin seams devoid of pegmatite (Fig. 9). In most of the situations, boudin axis are steeply west plunging (Fig. 10). Some complex fold structures in $S_{O/I}$ only occur adjacent to boudins in pegmatites. These boudin-related folds have variable styles and, in contrast to D_2 folds in the wall rock, variable vergence and orientation of axial surfaces and fold axes (Fig. 9). Locally, folds with opposite vergence occur facing each other across a boudin neck (a in Fig. 9). Because of their close connection to boudins, these folds probably formed during boudinage of the pegmatites as a result of the flow heterogeneity in the proximity of the boudins.

On horizontal outcrop faces, many pegmatites have contact zones in micaschist, up to 2 cm wide, that are enriched in tourmaline. Where pegmatite cuts though alternating micaschist and sandstone layers, tourmaline-rich rims are only developed in the micaschist. Tourmaline-rich rims are therefore interpreted as developing from boron-enriched fluids which invaded the wall rock of the veins, and transformed the mica in the micaschist into tourmaline. Within the tourmaline-rich rims, S_1 is preserved as a ghost foliation, made of tourmaline selvages and crystals.

In the higher strained zones, the ghost foliation in tourmaline-rich rims is commonly oblique to $S_{O/I}$ observed further away in the wall rock (Fig. 11a). This is especially obvious adjacent to the core of boudins, and in the wall rocks isolated in between branches of pegmatite veins (Fig. 11b). $S_{O/I}$ in the wall rock is continuous with the ghost foliation in the tourmaline-rich rims through folds that have axial planes parallel to the vein and fold axes parallel to L_2 in pegmatite. This fold structure can be explained by relative rotation of pegmatite dykes with their tourmaline-rich rims and $S_{O/I}$ in the wall rock during

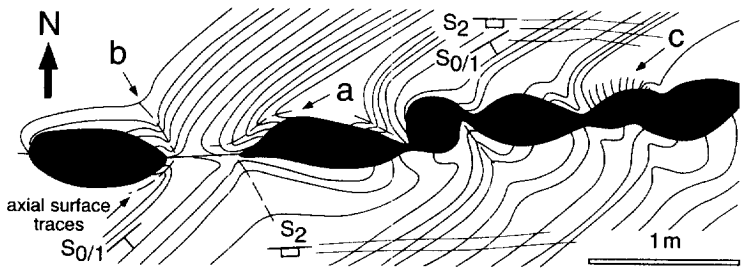

Fig. 9. Boudinaged pegmatite vein with complex fold structures in $S_{0/1}$. Details *a* and *b* refer to details in boudin-related folds described in the text. Detail *c* shows how $S_{0/1}$ is preserved in tourmaline-rich rims. S_2 is only developed further away from the pegmatite. Section is close to horizontal and located in Fig. 13.

D_2. The tourmaline-rich rims of the pegmatite dykes were probably more competent than the micaschist, and largely preserved an initial high angle between $S_{0/1}$ and the pegmatites when these intruded. Ductile flow in the micaschist changed the orientation between $S_{0/1}$ and pegmatites on a regional scale. Similar structures have been described on cm-scale around calcite veins in slate (Passchier and Urai, 1988).

The tourmaline-rich rim structures show that most pegmatites intruded subvertically oblique to $S_{0/1}$, although some dykes were emplaced parallel with bedding. Hence, several factors seem to govern the opening of the space occupied by the pegmatites. Oblique pegmatites were probably emplaced along tension fractures normal to the instantaneous extension direction, since there is no lateral displacement of markers over these planes. Other veins intruded parallel to $S_{0/1}$, indicating that this surface was also important mechanically as a plane of weakness.

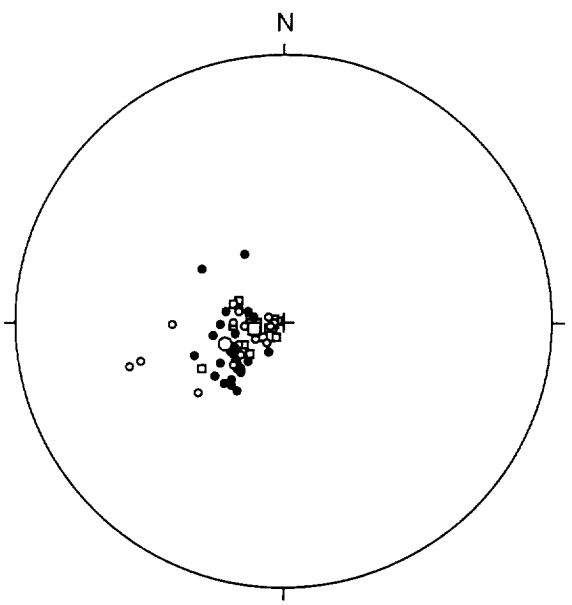

Fig. 10. Equal-area lower-hemisphere stereoplots showing the orientation of linear fabric elements in the Lighthouse area (shown in Figs. 1 and 13).○ = D_2 fold axes, □ = boudin axes, • = stretching lineations (L_2) in quartz (larger symbols mark mean vectors).

4. Kinematics of D_2

Shear zones are usually modelled as thin discs of intense deformation in less- to non-deformed parent rocks. Flow in such zones is thought to approximate simple shear which causes development of a planar and linear shape fabric with the linear component subparallel to the displacement direction at high strain. The non-coaxial nature of simple shear flow causes development of structures such as folds, asymmetric mantle porphyroclasts, mica-fish and shear band cleavage with a monoclinic shape symmetry, with the vorticity vector in the shape fabric plane, normal to the linear shape fabric component. This simple model seems to be valid in a majority of ductile shear zones described in the literature. As a result, the standard method to analyse displacement sense in ductile shear zones is as follows. First, the orientation of the linear component of the shape fabric or mineral lineation in the zone is established, assuming that it is parallel to the displacement direction at high strains. Second, sections normal to the shear zone and parallel to the lineations are used to find asymmetric structures; these are then interpreted in terms of shear sense.

In the study area, linear fabric elements such as

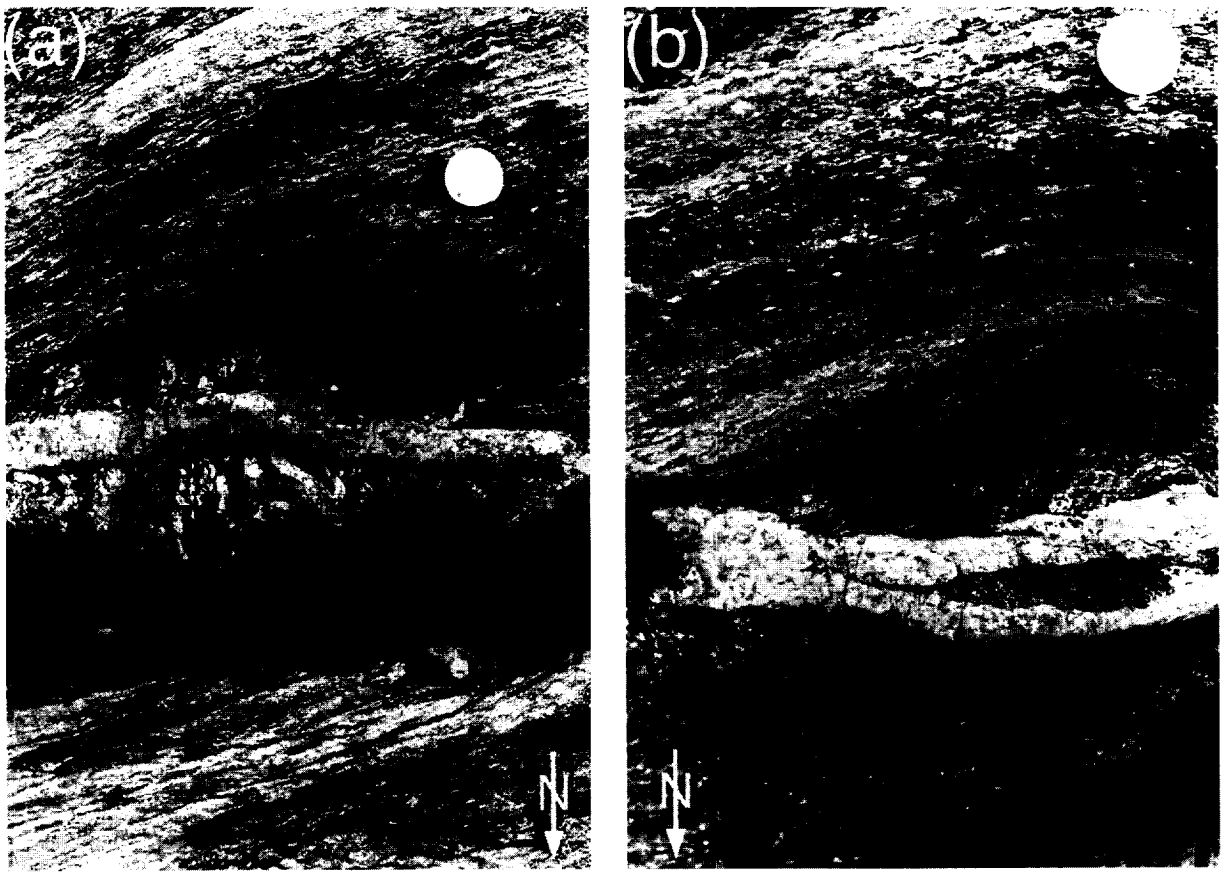

Fig. 11. Plane view field photographs of tourmaline-rich rims structures: (a) along a boudinaged pegmatite vein — $S_{O/I}$ is preserved in the rims at a high angle to the pegmatite walls; (b) along and in between branching pegmatite veins.

the linear component of the shape fabric, mineral lineations, intersection lineations, axes of cylindrical D_2 folds and axes of pegmatite boudins are subparallel and steeply west plunging (Fig. 10). However, most marked asymmetric structures are observed in gently dipping outcrop-sections normal or highly oblique to the stretching lineation, while only few asymmetries occur where they would be expected, i.e. on steeply west dipping rock faces normal to S_2 and parallel to the L_2. On these sections and all other steep faces all main structures are parallel and boudins are symmetrical.

Shear zones with lineations normal to the faces where asymmetric structures are observed have been described in other localities (Robin and Cruden, 1994). They could be explained in several ways.

(1) *All lineations are intersection lineations formed normal to the displacement direction of the shear zone.* Such structures might theoretically form in plane-strain simple shear zones. In the study area, this explanation seems unlikely; although some of the lineations in the area are certainly intersection lineations, which are parallel to mineral lineations and stretching lineations, and to the axes of cylindrical folds. It seems unlikely that such a constant relationship of linear fabric elements could develop normal to a displacement direction in simple shear. In that case, intersection lineations and fold axes would be expected to be wavy and varying in orientation. D_2 folds would not likely be strongly cylindrical.

(2) *The lineations and asymmetric structures were formed during two phases with displacement directions at right angles to each other.* Since deformation is never perfectly homogeneous but rather partitioned into low- and high-strain domains, such an overprint

would have variable effects on the older structures, and would particularly produce refolded folds and crenulation cleavage. In the study area, lineations and asymmetric structures have similar geometries and orientations and no overprint structures were found that could warrant two-phase event. This interpretation is therefore unlikely as well.

(3) *Flow was not simple shear, but was a non-coaxial flow that deviated from plane strain, with a strong stretching component parallel to the rotation (vorticity) axis of the flow.* Such flow types may be common in transpressive shear zones and produce a strain ellipsoid with the longest (X) axis parallel to the rotation axis (Sanderson and Marchini, 1984; Fossen and Tikoff, 1993; Robin and Cruden, 1994; Krantz, 1995). As a result, stretching and mineral lineation will be normal to the sections which display asymmetric structures. This model explains the data from the study area best. We therefore suggest that the high-strain zone in the study area was a non-plane strain sinistral transpressive shear zone with a strong stretching component vertically.

Stretching in a vertical direction, parallel to the rotation axis of flow can also explain some peculiarities of the pegmatites. Most pegmatites apparently intruded as steeply dipping dykes oblique to $S_{O/1}$. Since there is no offset of bedding and other markers parallel to the veins, they likely formed in tension, approximately parallel to a steep σ_2 and gently plunging σ_1. Because of the strong anisotropy of the parent rocks, σ_1 may have deviated from the orientation of the instantaneous shortening direction of ductile flow during D_2. The gently-dipping pegmatite branches (Fig. 6) result most likely from local reorientation of the stress field associated with a stretching component in the vertical direction. Subsequent deformation of these sheets is by folding with axes and axial planes parallel to S_2, which also fits vertical extension.

The subvertical attitude of boudin necks in pegmatites may seem to contradict the idea that vertical extension is important. Although some of the steeply dipping pegmatites appear slightly boudinaged in a vertical section, boudins with steep axes subparallel to the stretching lineation, observed in map view, seem dominant. In addition, in many outcrops the location of boudin necks coincides with psammitic layers. Since $S_{O/1}$ is vertical in the area, it is possible that this causes development of boudin axes parallel to the intersection line of pegmatites and $S_{O/1}$ (Talbot, 1970).

4.1. Kinematic analysis in the vorticity profile plane

Several structures in the horizontal plane, which constitutes a section close-parallel to the vorticity profile plane (Robin and Cruden, 1994), indicate that shear sense was sinistral, i.e. the geometry of sigmoidal quartz-rods, the geometry of asymmetric D_2 folds, the inclusion pattern in porphyroblasts, the orientation of pegmatite boudins with respect to the pegmatite vein enveloping surface and the distribution of folded and boudinaged pegmatites in space (Fig. 6 and Passchier, 1990). Unfortunately, strain is rather inhomogeneously distributed over the area, which inhibits a quantitative kinematic approach.

In any progressive deformation, a line or plane can be defined towards which material lines, and consequently foliations and lineations rotate: in simple shear this is the flow plane, but similar planes and lines exist in other types of progressive deformation. We name such lines and planes 'fabric attractors' (following Passchier and Trouw, 1995, p. 19).

The angle between $S_{O/1}$ and S_2 decreases with increasing strain in the area, and this implies rotation of these surfaces towards the fabric attractor. In the core of the high-strain zone, both fabric elements are nearly parallel, hence close to the orientation of the fabric attractor.

Elongate rigid ellipsoids in a homogeneously deforming fluid will show a complex rotation behaviour, depending on the length/width ratio of the object, the vorticity of the flow and finite strain (Passchier, 1987). In principle, all objects except infinitely long ones rotate permanently in simple shear; the latter are blocked by the fabric attractor (Passchier, 1987; Passchier and Trouw, 1995, p. 119). In non-coaxial flows between pure and simple shear, only stocky objects rotate, while more elongate ones rotate over a small angle to a blocking orientation that depends on the shape of the object. In practice, blocked elongate objects will make a small (5–25°) angle with blocked infinitely long objects (Passchier, 1987; Passchier and Trouw, 1995, fig. 5.23). Although sigmoidal quartz-rods deviate from a rigid

ellipsoid model, a plot of their rotation angle (α) with respect to their length–width ratio (R) shows a distribution similar to that expected for ellipsoids (Fig. 5). The orientation distribution of sigmoidal quartz-rods indicates that flow was probably highly vortical, close to simple shear, but with a pure shear component.

The tourmaline-rich rim-structures described above give information on the relative rotation of $S_{O/I}$ and pegmatites. In the medium strain zone of the study area, relative rotation up to 110° with a remaining angle between boudinaged pegmatites and $S_{O/I}$ of 30° has been observed. Assuming that the pegmatites intruded in an orientation near the bulk shortening direction during D_2 flow, rotations of 90° (pure shear) to 135° simple shear are possible towards the fabric attractor. A rotation angle of 110° therefore agrees with a highly vortical flow.

4.2. Strain characterisation in the vorticity profile plane

Sets of differently oriented quartz-veins and pegmatite dykes have been used to determine the stretch values and the related D_2 strain ellipse in map view. Each outcrop selected for analysis shows a rather homogeneous deformation with constant orientations of S_1 and S_2. While the early quartz-veins record the bulk D_2 deformation, the pegmatite sets came later on, so they record only part of the D_2 deformation, i.e. the strain post-dating their emplacement. Bulk D_2 strain determinations have not been performed in higher strain domains because all earlier structures become into close parallelism, impeding their use in strain analysis.

Fig. 12 shows strain ellipses determined by this method, allowing to determine the local strain ratio (R) and area-change. The axial ratios on the outcrop

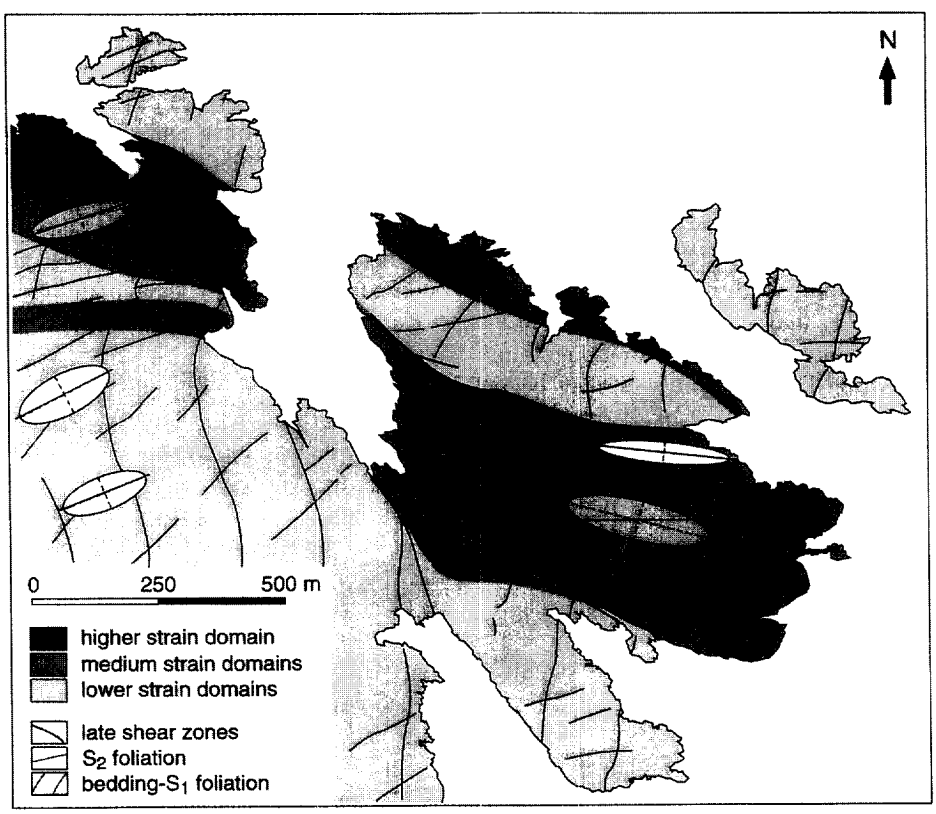

Fig. 12. Sketch map of the Culip–Cap de Creus area showing the arrangement of different structural domains and some sectional ellipses. In white: bulk D_2 strains recorded by early quartz-veins; in grey: strain recorded by pegmatites.

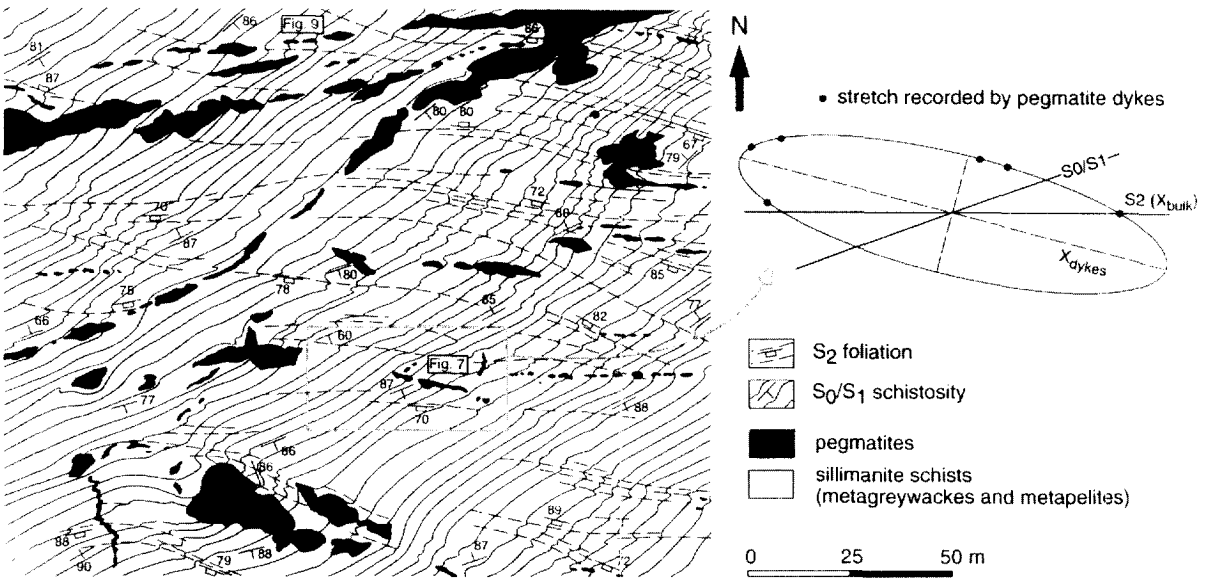

Fig. 13. Detail map from the Lighthouse area with differently oriented pegmatites in the medium strain domain. A sectional strain ellipse has been plotted from pegmatite stretch data, showing the obliquity of the long axis of this ellipse and the trace of the S_2 crenulation foliation which tracks the X-axis of the bulk D_2 sectional ellipse.

surface found in low-strain domains range between ($R = 2.3$ and $R = 2.8$). They are sectional ellipse values and consequently represent lower values than those corresponding to the X/Z ratio of the strain ellipsoid which is expected to lie in subvertical planes, but cannot be measured accurately.

The strain recorded by the pegmatites is consistently lower than the bulk strain recorded in the mica-schists in medium strain domains (Fig. 12). This is not only indicated by the recorded strain values but also by the difference in tightness of coaxially folded schists and pegmatites and from comparison of strain values recorded in schists from low-strain domains with strains recorded in pegmatites in medium strain domains (strain ratios between $R = 3.5$ and $R = 3.7$). These observations are in agreement with the proposed synkinematic nature of the pegmatites.

Another significant result is the obliquity of the long axis of the calculated ellipses with the orientation of S_2, i.e. the long axis of the bulk strain ellipses (Fig. 13). This fact evidences the non-coaxiallity of the deformation, being the bulk strain ellipse sinistrally rotated with regard to the lower strain ellipse recorded by the pegmatite dykes.

5. Discussion and conclusions

Although small-scale structures indicate sinistral shear sense in the high-strain zone, the map view of high- and low-strain zones (Figs. 1 and 3) shows a deflection of $S_{O/I}$ into the high-strain zone that may seem difficult to reconcile with a sinistral shear sense.

Most shear zones, including these developing by simple shear and transpression, have the fabric attractor oriented parallel to the shear zone boundary: as a result, internal shear sense and displacement sense of external markers over the shear zone are identical.

We propose (Fig. 14) that the high-strain zone in the Cap de Creus area did not form with the fabric attractor parallel to the boundaries of high- and low-strain zones. As discussed above, the high-strain zone is probably a zone of highly vortical sinistral non-coaxial flow with a strong vertical extension component. If no major volume change is involved, the shear zone was probably thinning in order to compensate for vertical extension. The fabric attractor was apparently close to the $S_{O/I}$ plane at the end of D_2. Since asymmetric D_2 structures

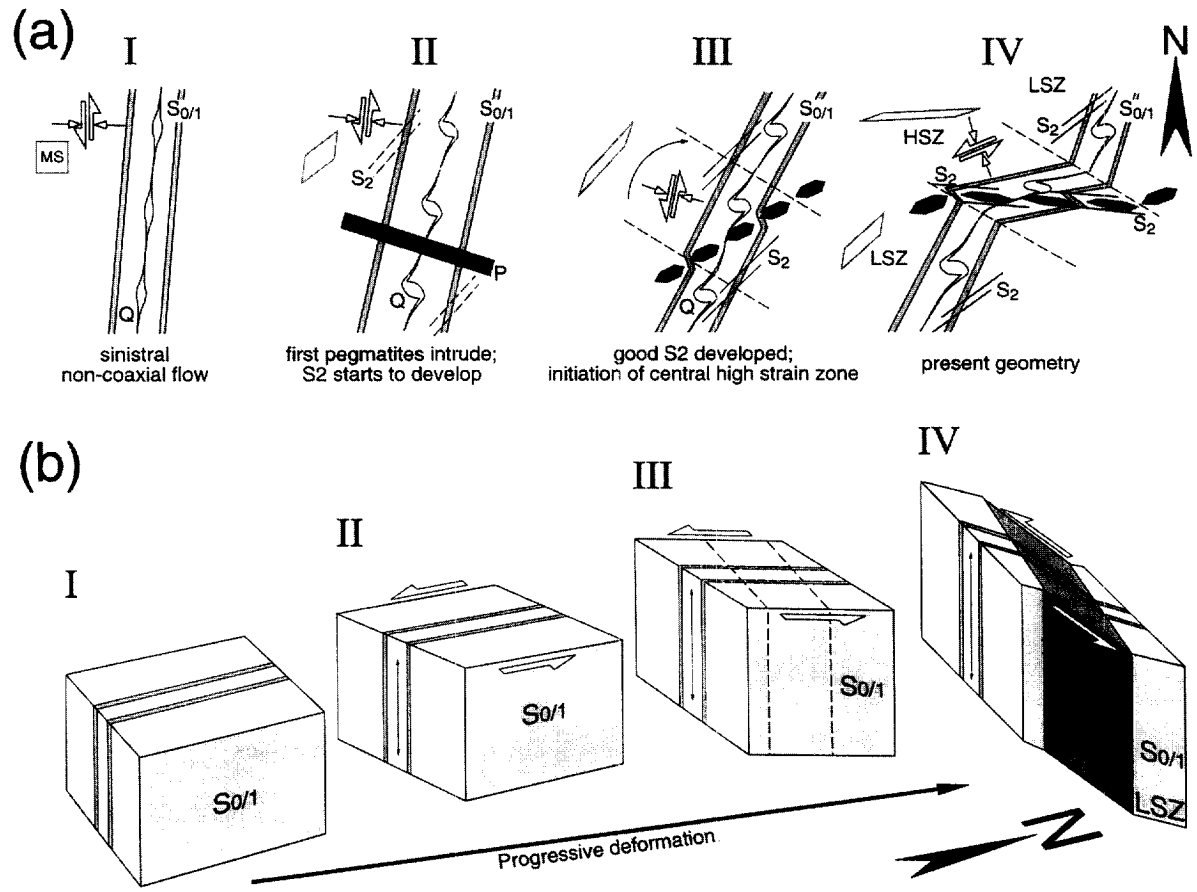

Fig. 14. Sketches of the sequence of events leading to the present geometry of D_2 structures in the Cap de Creus area, in map view (a) and in block diagram (b). Stage I: pre-D_2 structure of boudinaged quartz-veins (*Q*) subparallel to $S_{0/1}$. *MS* is a marker square. Arrows indicate orientation of the kinematic frame. Stage II: D_2 sinistral non-coaxial flow causes rotation of the quartz-boudins to produce sigmoidal quartz-rods and incipient S_2. Pegmatites (*P*) intrude approximately normal to $S_{0/1}$. Stage III: continued deformation leads to strain of pegmatites and further development of S_2 and sigmoidal quartz-rods. Stage IV: further deformation is concentrated in the high-strain zone (*HSZ*), leading to development of the dextral flexure. *LSZ* = low-strain zone. Notice vertical extension during D_2 progressive deformation (vertical arrows in block diagrams).

are present in both the high- and low-strain zones, it is likely that similar flow took place in both zones, but that deformation either continued longer in the high-strain zone, or that strain rate was higher there. In any case, since the fabric attractor was at a small angle to $S_{0/1}$ at the end of D_2, it must have been oblique to the boundary of the high-strain zone. This implies that the high-strain zone is not a shear zone in the classical sense, with a fabric attractor parallel to zone boundaries. Sinistral non-coaxial flow in the high-strain zone may have caused a dextral flexure of $S_{0/1}$ if flow in the low-strain zones was either slower or earlier that in the high-strain core (Fig. 14). This mechanism is similar to that of flexural flow in a fold. We did not use the term flexural flow here, however, since this strictly implies simple shear parallel to bedding, which does not exactly fit the kinematic regime determined for the Cap de Creus area.

The Cap de Creus area contains an unusual high-strain zone developed at medium- to high-metamorphic grades that seems to have developed by transcurrent sinistral non-coaxial flow, combined with vertical extension (Fig. 14). Stretching and mineral

lineations are steep and developed in a direction normal to the sinistral 'displacement' direction in the high-strain zone. Most asymmetric shear sense indicators occur on horizontal outcrop faces normal to the lineations. Nevertheless, the high-strain zone cannot be described as a simple transpressive shear zone. Transpressive deformation has its fabric attractor parallel to the shear zone, as in simple shear and nearly all other modelled shear zones. Sinistral shear sense indicators in the Cap de Creus area seem to be in conflict with a 'dextral' deflection of older foliations over the high-strain zone, and this geometry can be explained by a flow regime with a fabric attractor oblique to the shear zone. It seems, therefore, possible that ductile shear zones with sinistral shear sense produce a dextral deflection of an older foliation. In medium- to high-grade zones it is, therefore, necessary to be careful when interpreting lineations in terms of displacement direction, and with the interpretation of deflection of older fabric elements into high-strain zones.

Acknowledgements

Financial support for this work by DAAD (Nrs. 322-AI-e-dr and 155B). C.W.P., P.V. and B.D.B. gratefully acknowledge the Volkswagen Stiftung. The research of E.D. and J.C. was also sponsored by DGCICYT Proyecto: PB 91-0477.

References

Alfonso, M.P., 1995. Aproximación a la petrogénesis de las pegmatitas del Cap de Creus. Unpublished thesis, Universitat de Barcelona, 388 pp.

Carreras, J., Casas, J.M., 1987. On folding and shear zone development: a mesoscale structural study on the transition between two different tectonic styles. Tectonophysics 135, 87–98.

Carreras, J., Druguet, E., 1994. Structural zonation as a result of inhomogeneous non-coaxial deformation and its control on syntectonic intrusions: an example from the Cap de Creus area (eastern-Pyrenees). J. Struct. Geol. 16, 1525–1534.

Druguet, E., Enrique, P., Galán, G., 1995. Tipología de los granitoides y rocas asociadas del complejo migmatítico de la Punta dels Farallons (Cap de Creus, Pirineo Oriental). Geogaceta 18, 199–202.

Fossen, H., Tikoff, B., 1993. The deformation matrix for simultaneous simple shearing, pure shearing, and volume change, and its application to transpression–transtension tectonics. J. Struct. Geol. 15, 413–422.

Hutton, D.H.W., 1988. Granite emplacement mechanisms and tectonic controls: inferences from deformation studies. Trans. R. Soc. Edinburgh 79, 245–255.

Ingram, G.M., Hutton, D.H.W., 1994. The great Tonalite Sill: Emplacement into a contractional shear zone and implications for Late Cretaceous to early Eocene tectonics in southeastern Alaska and British Columbia. Bull. Geol. Soc. Am. 106, 715–728.

Karlstrom, K.E., Williams, M.L., 1995. The case for simultaneous deformation, metamorphism and plutonism: an example from Proterozoic rocks in central Arizona. J. Struct. Geol. 17, 59–81.

Krantz, R.W., 1995. The transpressional strain model applied to strike-slip, oblique-convergent and oblique-divergent deformation. J. Struct. Geol. 17, 1125–1137.

McCaffrey, K.J.W., 1994. Magmatic and solid state deformation partitioning in the Ox Mountains granodiorite. Geol. Mag. 131, 639–652.

Means, W.D., Hobbs, B.E., Lister, G.S., Williams, P.F., 1980. Vorticity and non-coaxiallity in progressive deformations. J. Struct. Geol. 2, 371–378.

Passchier, C.W., 1987. Stable positions of rigid objects in non-coaxial flow: a study in vorticity analysis. J. Struct. Geol. 9, 679–690.

Passchier, C.W., 1990. Reconstruction of deformation and flow parameters from deformed vein sets. Tectonophysics 180, 185–199.

Passchier, C.W., Trouw, R.A.J., 1995. Microtectonics. Springer, Heidelberg.

Passchier, C.W., Urai, J.L., 1988. Vorticity and strain analysis using Mohr diagrams. J. Struct. Geol. 10, 755–763.

Ramsay, J.G., 1980. Shear zone geometry: a review. J. Struct. Geol. 2, 83–99.

Reavy, R.J., 1989. Structural controls on metamorphism and syn-tectonic magmatism: the Portuguese Hercynian collision belt. J. Geol. Soc. London 146, 649–657.

Robin, P.Y.F., Cruden, A.R., 1994. Strain and vorticity patterns in ideally ductile transpression zones. J. Struct. Geol. 16, 447–466.

Sanderson, D.J., Marchini, W.R.D., 1984. Transpression. J. Struct. Geol. 6, 449–458.

Talbot, C.J., 1970. The minimum strain ellipsoid using deformed quartz veins. Tectonophysics 9, 47–76.